Volume 51 | Number 16 | 25 February 2015 | Pages 3275–3476

ChemComm

Chemical Communications

www.rsc.org/chemcomm

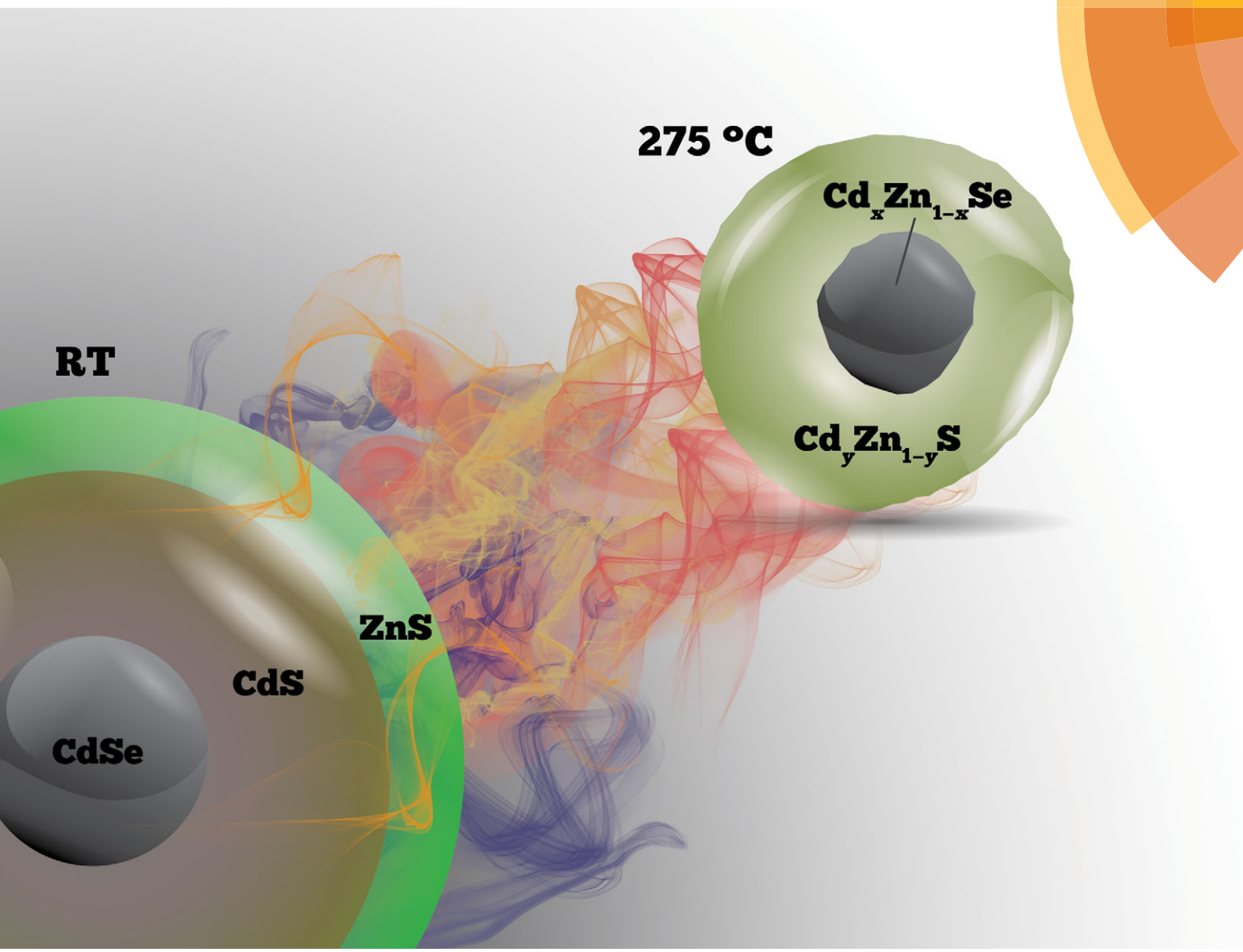

ISSN 1359-7345

ROYAL SOCIETY OF CHEMISTRY

COMMUNICATION

Anil O. Yalcin *et al.*

Heat-induced transformation of CdSe–CdS–ZnS core–multishell quantum dots by Zn diffusion into inner layers

ChemComm

COMMUNICATION

View Article Online
View Journal | View Issue

Cite this: *Chem. Commun.*, 2015, **51**, 3320

Received 31st October 2014,
Accepted 21st November 2014

DOI: 10.1039/c4cc08647c

www.rsc.org/chemcomm

Heat-induced transformation of CdSe–CdS–ZnS core–multishell quantum dots by Zn diffusion into inner layers†

Anil O. Yalcin,*[a] Bart Goris,[b] Relinde J. A. van Dijk-Moes,[c] Zhaochuan Fan,[d] Ahmet K. Erdamar,[a] Frans D. Tichelaar,[a] Thijs J. H. Vlugt,[d] Gustaaf Van Tendeloo,[b] Sara Bals,[b] Daniël Vanmaekelbergh,[c] Henny W. Zandbergen[a] and Marijn A. van Huis[e]

In this work, we investigate the thermal evolution of CdSe–CdS–ZnS core–multishell quantum dots (QDs) *in situ* using transmission electron microscopy (TEM). Starting at a temperature of approximately 250 °C, Zn diffusion into inner layers takes place together with simultaneous evaporation of particularly Cd and S. As a result of this transformation, $Cd_xZn_{1-x}Se$–$Cd_yZn_{1-y}S$ core–shell QDs are obtained.

CdSe, a II–VI type semiconductor, is a widely studied nanocrystal (NC) in colloidal science as its emission can cover the whole visible spectrum *via* size tuning,[1,2] making CdSe NCs important for several applications such as biolabeling and LEDs.[3,4] Despite having interesting functional properties, NCs in general suffer from instability, in particular surface oxidation,[5,6] due to the high surface to volume ratio. In order to increase the stability of CdSe QDs, a wide-band gap II–VI semiconductor such as ZnS can be successfully grown onto a CdSe core. The advantage of a wide-band gap ZnS shell is that both electrons and holes are kept confined in the core with increased stability as well as decreased toxicity.[7–10] However, the lattice mismatch in the CdSe–ZnS core–shell system is about 12%, leading to interfacial strain, thus resulting in the formation of trap sites for charge carriers and increased blinking.[1,8,11–13] In order to overcome this problem, an intermediate layer of CdS with a lattice constant between CdSe and ZnS can be incorporated into the structure.[7,14–16] With this CdS intermediate layer, the interfacial strain is reduced and the optical properties are enhanced.[7,14–16] We thus speak of CdSe–CdS–ZnS core–multishell QDs.

Although the knowledge of the synthesis of NCs as well as the optical properties of NCs is now advanced, detailed information on the thermal and temporal behavior of these structures is limited. *In situ* transmission electron microscopy (TEM) coupled with the microelectronic mechanical system (MEMS) technology can shed light on various interesting thermal changes in nanostructures, which can be of critical importance for the implementation of these QDs in devices. For example, in CdSe–CdS dot-in-octapod morphology NCs, heating induces the segregation of pure Cd domains at the side of the octapods.[17] In another work, the Fe_xO–$CoFe_2O_4$ core–shell system undergoes a temperature-induced reconfiguration whereby Fe_xO leaves the core location and segregates at the side of the $CoFe_2O_4$ domain while $CoFe_2O_4$ shrinks and fills the core volume.[18]

Here, we show the thermal evolution of CdSe–CdS–ZnS core–multishell QDs whereby Zn diffusion into the inner layers of the QDs takes place at elevated temperatures. The structure evolves into $Cd_xZn_{1-x}Se$–$Cd_yZn_{1-y}S$ core–shell QDs with irregular morphologies.

The synthesis of the CdSe–CdS–ZnS colloidal QDs was performed as follows: CdSe QD seeds were synthesized first,[19] and then a CdS–ZnS multishell was grown onto CdSe QD seeds *via* the successive ion layer adhesion and reaction (SILAR) method.[7] In order to minimize the interfacial strain between the CdS and ZnS shells, a monolayer of CdZnS was grown in between. Details about the synthesis can be found in the ESI.† For *in situ* heating experiments, 8 μL of colloidal QD solution was deposited on a MEMS based micro-hotplate inside an argon-atmosphere glove box. After the evaporation of the solvent, the set-up was mounted on a low drift heating holder produced by DENSsolutions.[20] The *in situ* heating experiments were conducted using two different Cs-corrected FEI Titan microscopes, one of which is equipped with a high-brightness gun and a Chemi-STEM (Scanning Transmission Electron Microscopy) detection system for Energy Dispersive X-ray Spectroscopy (EDX). Both Bright Field TEM (BF-TEM) and High Angle Annular Dark Field STEM (HAADF-STEM) imaging techniques were used in our studies. In order to prevent beam damage while using the high-brightness gun in Chemi-STEM

[a] *Kavli Institute of Nanoscience, Delft University of Technology, Lorentzweg 1, 2628 CJ Delft, The Netherlands. E-mail: a.o.yalcin@tudelft.nl*
[b] *Electron Microscopy for Materials Science (EMAT), University of Antwerp, Groenenborgerlaan 171, 2020 Antwerp, Belgium*
[c] *Condensed Matter and Interfaces, Debye Institute for Nanomaterials Science, Utrecht University, Princetonplein 5, 3584 CC Utrecht, The Netherlands*
[d] *Process and Energy Laboratory, Delft University of Technology, Leeghwaterstraat 39, 2628 CB Delft, The Netherlands*
[e] *Debye Institute for Nanomaterials Science, Center for Extreme Matter and Emergent Phenomena, Utrecht University, Princetonplein 5, 3584 CC Utrecht, The Netherlands*

† Electronic supplementary information (ESI) available: The synthesis method of CdSe–CdS–ZnS core–multishell QDs, STEM-EDX elemental maps at different temperatures, elemental quantifications, and Movies S1 and S2. See DOI: 10.1039/c4cc08647c

elemental map studies, a relatively low acceleration voltage of 120 kV was employed. Other studies were carried out at an acceleration voltage of 300 kV. A camera length of 115 mm was used in HAADF-STEM studies to limit diffraction effects in this mode.

Fig. 1a presents an HAADF-STEM projection of several CdSe–CdS–ZnS core–multishell QDs in their initial state at room temperature (RT). The corresponding elemental maps of Se, S, Cd and Zn are displayed in Fig. 1b–e, and an overlay of the Cd and the Zn map is presented in Fig. 1f. From the maps, it is clear that the QDs consist of a CdSe core, a CdS intermediate layer and a ZnS outer shell. The Se-map (Fig. 1b) as well as the empty QD centers in the S-map (Fig. 1c) indicate the CdSe core region. The overlay of the Cd- and Zn-maps (Fig. 1f) clearly demonstrates the outer shell. From the elemental quantifications performed on 10 different QDs (Table S2 in the ESI†), the average cation/anion ratio was found to be 0.99 ± 0.05 throughout the structure. All elemental quantifications were performed using the Cliff–Lorimer method with *k*-factors as implemented in the Bruker ESPRIT software. Fig. 1g and h show high resolution (HR) TEM images of two QDs along [001] and [1$\bar{1}$0] zones, respectively. From the HRTEM images and inset Fourier Transforms (FTs), the crystal structure was found to be hexagonal wurtzite. HRTEM images did not show any defects or irregularities throughout the structure, showing that the CdS–ZnS shell was grown epitaxially on CdSe.[7,15] The FTs do not reveal separate atomic spacings of different layers. It has been reported that in the CdSe–CdS core–shell and the CdSe–CdS–ZnS core–multishell systems, the CdSe core is compressed by the shell domains.[15,21] As a result, the atomic spacings of CdSe are reduced. From the FTs, we observed the atomic spacings close to that of CdS as most of the QD is composed of the CdS intermediate layer and therefore dominating the structural properties of the QDs as a whole.

When CdSe–CdS–ZnS core–multishell QDs were heated in the TEM, we observed a morphological and structural change as depicted in Fig. 2. The initial sphere-like QDs adopted irregular shapes starting at temperatures of 250 °C and higher. Movie S1 (ESI†) shows the morphological evolution of QDs when they were heated from 200 °C up to the sublimation temperature of 320 °C. Considering the elemental distribution, Fig. 2 shows that Zn diffused into the inner layers of the QD structure. The high temperature Zn-map (Fig. 2e) covered the QD structures completely, which was not the case at the initial state (Fig. 1e) where Zn was only present in the outer shell. Note that chemical mapping was always performed in areas not previously exposed to the electron beam, and the transformation was found to take place on the entire TEM support membrane, indicating that the electron beam did not initiate the transformation. In the literature, Zn diffusion has been observed in CdSe–ZnSe[22–24] and $Cd_{1-x}Zn_xS$–ZnS core–shell structures[25,26] at elevated temperatures. It has been reported that cations in II–VI semiconductors such as ZnS have a high tendency to diffuse.[27–29] Considering the anions, the Se-map (Fig. 2b) shows that Se retains its position in the core at high temperature. Moreover, the QD centers in the S-maps (Fig. 2c) are still dark, indicating that S did not diffuse into the core. Note that besides the change in the structure and morphology, the overall size of the QDs became smaller at elevated temperature due to simultaneous evaporation

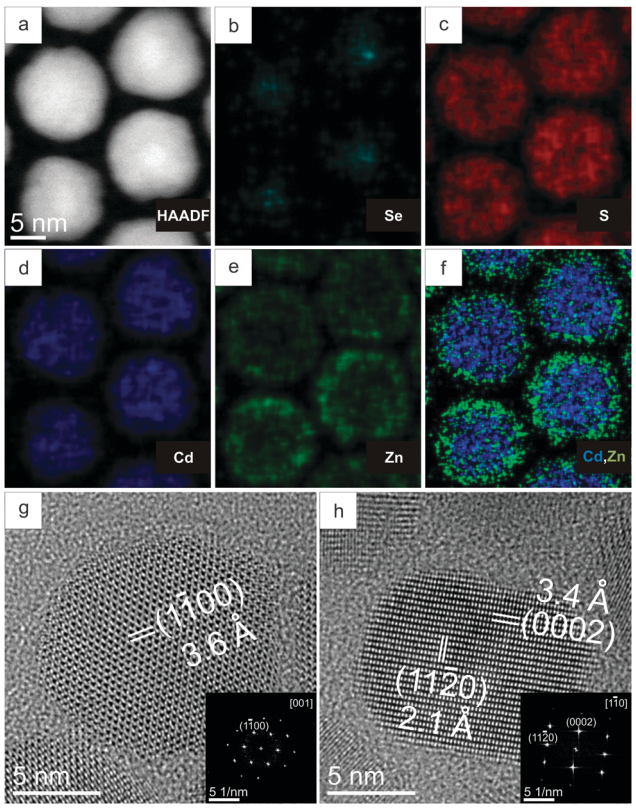

Fig. 1 (a) HAADF-STEM image of CdSe–CdS–ZnS core–multishell QDs at their initial state at RT. (b–f) The corresponding Se, S, Cd and Zn elemental maps and an overlay of the Cd and Zn elemental maps obtained by EDX mapping. The scale bar in (a) applies also to (b–f). (g and h) HRTEM images of two QDs along two different zone axes.

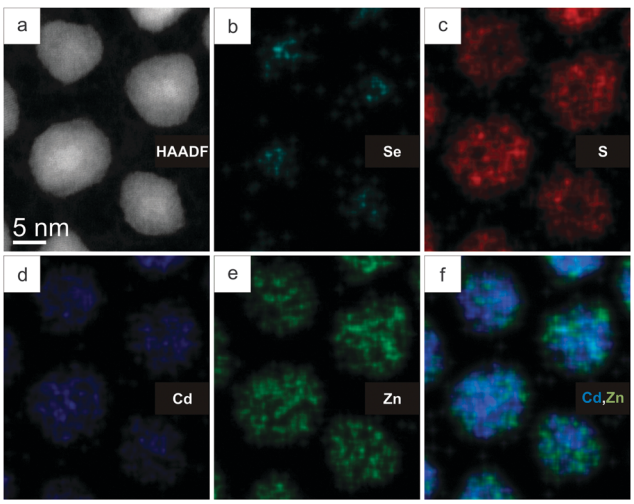

Fig. 2 (a) HAADF-STEM image of QDs at 275 °C. (b–f) The corresponding Se, S, Cd and Zn elemental maps and an overlay of the Cd and Zn elemental maps obtained by EDX mapping. Elemental maps indicate that CdSe–CdS–ZnS QDs transformed into $Cd_xZn_{1-x}Se$–$Cd_yZn_{1-y}S$ core–shell structures by Zn diffusion into the inner layers. The scale bar in (a) applies also to (b–f).

of cation and anion species. The cation/anion ratio obtained through elemental quantification of 10 different QDs verifies this (Table S3 in the ESI†). At elevated temperature, the average cation/anion ratio was found to be 0.96 ± 0.08, which is similar to the ratio at the initial state. In order for this to happen, simultaneous sublimation of species (particularly Cd and S) should take place, so that Zn can replace some Cd in CdS and CdSe. Unless the in-diffusing Zn atoms all occupy interstitial sites, the in-diffusion of Zn is accompanied by out-diffusion of part of the Cd atoms and subsequent evaporation. The diffusion process could be either a vacancy-assisted migration mechanism,[30] or an interstitial-substitutional migration mechanism.[31]

From the quantifications, the average Cd content in the whole QD decreased from 38 at% to 27 at% and the average Zn content increased from 12 at% to 22 at%, suggesting the evaporation of Cd with heating. We mention here that the vapour pressure of pure Cd is two orders of magnitude higher than that of pure Zn in this temperature range,[32] but the evaporation from the QD also depends on the bond strengths of the compounds. Cd evaporation from heterogeneous NCs was previously observed when sandwich morphology CdSe–Cu_3P–CdSe NCs were heated.[33] Recently, we also observed Cd evaporation in CdSe–PbSe heterogeneous NCs at temperatures even lower than 200 °C.[30] The average atomic percentages of anions (Se and S) in the QDs did not change much with heating. As the average cation/anion ratio after transformation was found to be 0.96 ± 0.08 (still close to 1), not only cations but also anions should have evaporated during heating. In summary, as a result of *in situ* heating, CdSe–CdS–ZnS core–multishell QDs transformed into two-layer $Cd_xZn_{1-x}Se$–$Cd_yZn_{1-y}S$ core–shell QDs.

To monitor the effect of heating on the crystal structure, the evolution of a single QD was followed in high resolution. Fig. 3 shows high resolution HAADF-STEM images of a single QD at different temperatures until the sublimation at 310 °C. The QD was oriented along the [001] projection (along the *c*-axis). The FT of each image in Fig. 3 is placed below each corresponding image. The QD retained the hexagonal wurtzite crystal structure up to the sublimation point. At a temperature of 270 °C (Fig. 3b), a dark spot in the middle of a QD was observed, possibly due to the accumulation of radiation damage caused by the focused electron beam during imaging in high resolution. Note that the 'parking position' of the electron probe was far away from the QD in order to limit beam induced damage. Movie S2 (ESI†) shows the QD shown in Fig. 3 at the later stages of heating and while undergoing partial sublimation. With heating, the morphology of the QD changed at first and a significant part of the QD sublimated later.

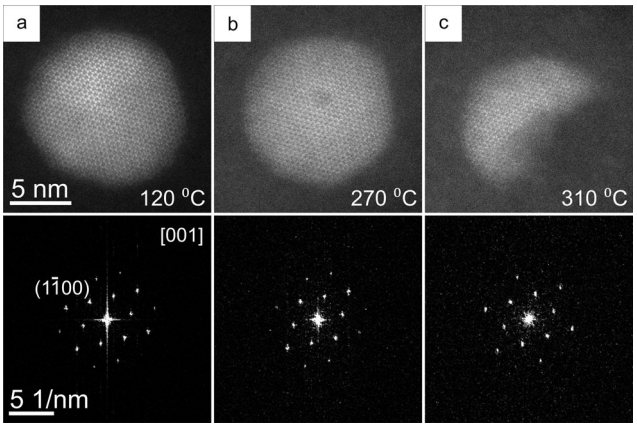

Fig. 3 High resolution HAADF-STEM study of a QD during thermal evolution at temperatures of (a) 120 °C, (b) 270 °C, and (c) 310 °C. The FT of each image is placed below the image. The scale bars in (a) and in the corresponding FT apply to all images and FTs.

In this study, we have shown *in situ* the thermal evolution of CdSe–CdS–ZnS core–multishell QDs into $Cd_xZn_{1-x}Se$–$Cd_yZn_{1-y}S$ core–shell QDs by Zn diffusion into the inner layers of the QDs starting from approximately 250 °C. The initial sphere-like morphology of the QDs became irregular upon heat treatment and the QDs became smaller in size due to simultaneous evaporation of cation and anion species (particularly Cd and S). High resolution HAADF-STEM studies revealed that the hexagonal wurtzite crystal structure was retained up to the sublimation point.

This work is part of the research programme of the Foundation for Fundamental Research on Matter (FOM), which is part of the Netherlands Organization for Scientific Research (NWO). European Soft Matter Infrastructure (ESMI) is acknowledged for the Transnational Access Grant. M.A.v.H. acknowledges a VIDI grant from NWO. B.G. acknowledges the Flemish Research Foundation (FWO Vlaanderen). G.V.T. and S.B. acknowledge funding from the European Research Council (ERC) under the Seventh Framework Program (FP7), ERC Grant No. 246791-Countatoms and ERC Grant No. 335078-Colouratom.

Notes and references

1 D. V. Talapin, I. Mekis, S. Götzinger, A. Kornowski, O. Benson and H. Weller, *J. Phys. Chem. B*, 2004, **108**, 18826.
2 S. A. Empedocles and M. G. Bawendi, *Science*, 1997, **278**, 2114.
3 A. Samanta, Z. Deng and Y. Liu, *Langmuir*, 2012, **28**, 8205.
4 A. M. Munro and D. S. Ginger, *Nano Lett.*, 2008, **8**, 2585.
5 B. De Geyter and Z. Hens, *Appl. Phys. Lett.*, 2010, **97**, 161908.
6 R. C. Somers, M. G. Bawendi and D. G. Nocera, *Chem. Soc. Rev.*, 2007, **36**, 579.
7 R. Xie, U. Kolb, J. Li, T. Basché and A. Mews, *J. Am. Chem. Soc.*, 2005, **127**, 7480.
8 S. Xu, H. Shen, C. Zhou, H. Yuan, C. Liu, H. Wang, L. Ma and L. S. Li, *J. Phys. Chem. C*, 2011, **115**, 20876.
9 H. Shen, S. Wang, H. Wang, J. Niu, L. Qian, Y. Yang, A. Titov, J. Hyvonen, Y. Zhen and L. S. Li, *ACS Appl. Mater. Interfaces*, 2013, **5**, 4260.
10 K. Kim, C. J. Han, Y. C. Park, Isnaeni, Y.-H. Cho and S. Jeong, *Nanotechnology*, 2013, **24**, 505601.
11 X. Wang, X. Ren, K. Kahen, M. A. Hahn, M. Rajeswaran, S. Maccagnano-Zacher, J. Silcox, G. E. Cragg, A. L. Efros and T. D. Krauss, *Nature*, 2009, **459**, 686.
12 B. Mahler, P. Spinicelli, S. Buil, X. Quelin, J.-P. Hermier and B. Dubertret, *Nat. Mater.*, 2008, **7**, 659.
13 H. Shen, H. Wang, C. Zhou, J. Z. Niu, H. Yuan, L. Ma and L. S. Li, *Dalton Trans.*, 2011, **40**, 9180.
14 X. Wang, W. Li and K. Sun, *J. Mater. Chem.*, 2011, **21**, 8558.
15 L. Manna, E. C. Scher, L.-S. Li and A. P. Alivisatos, *J. Am. Chem. Soc.*, 2002, **124**, 7136.
16 S. Deka, A. Quarta, M. G. Lupo, A. Falqui, S. Boninelli, C. Giannini, G. Morello, M. De Giorgi, G. Lanzani, C. Spinella, R. Cingolani, T. Pellegrino and L. Manna, *J. Am. Chem. Soc.*, 2009, **131**, 2948.
17 B. Goris, M. A. van Huis, S. Bals, H. W. Zandbergen, L. Manna and G. Van Tendeloo, *Small*, 2012, **8**, 937.
18 A. O. Yalcin, B. de Nijs, Z. Fan, F. D. Tichelaar, D. Vanmaekelbergh, A. van Blaaderen, T. J. H. Vlugt, M. A. van Huis and H. W. Zandbergen, *Nanotechnology*, 2014, **25**, 055601.

19 X. Peng, M. C. Schlamp, A. V. Kadavanich and A. P. Alivisatos, *J. Am. Chem. Soc.*, 1997, **119**, 7019.
20 M. A. van Huis, N. P. Young, G. Pandraud, J. F. Creemer, D. Vanmaekelbergh, A. I. Kirkland and H. W. Zandbergen, *Adv. Mater.*, 2009, **21**, 4992.
21 N. Tschirner, H. Lange, A. Schliwa, A. Biermann, C. Thomsen, K. Lambert, R. Gomes and Z. Hens, *Chem. Mater.*, 2012, **24**, 311.
22 Y.-M. Sung, Y.-J. Lee and K.-S. Park, *J. Am. Chem. Soc.*, 2006, **128**, 9002.
23 K. G. Sonawane, K. R. Patil and S. Mahamuni, *J. Lumin.*, 2013, **135**, 154.
24 H. Lee, P. H. Holloway and H. Yang, *J. Chem. Phys.*, 2006, **125**, 164711.
25 W. K. Bae, M. K. Nam, K. Char and S. Lee, *Chem. Mater.*, 2008, **20**, 5307.
26 X. Liu, Y. Jiang, F. Fu, W. Guo, W. Huang and L. Li, *Mater. Sci. Semicond. Process.*, 2013, **16**, 1723.
27 K. Boldt, N. Kirkwood, G. A. Beane and P. Mulvaney, *Chem. Mater.*, 2013, **25**, 4731.
28 X. Zhong, M. Han, Z. Dong, T. J. White and W. Knoll, *J. Am. Chem. Soc.*, 2003, **125**, 8589.
29 J. Xu, X. Yang, H. Wang, X. Chen, C. Luan, Z. Xu, Z. Lu, V. A. L. Roy, W. Zhang and C.-S. Lee, *Nano Lett.*, 2011, **11**, 4138.
30 A. O. Yalcin, Z. Fan, B. Goris, W.-F. Li, R. S. Koster, C.-M. Fang, A. van Blaaderen, M. Casavola, F. D. Tichelaar, S. Bals, G. Van Tendeloo, T. J. H. Vlugt, D. Vanmaekelbergh, H. W. Zandbergen and M. A. van Huis, *Nano Lett.*, 2014, **14**, 3661.
31 F. D. Ott, L. L. Spiegel, D. J. Norris and S. C. Erwin, *Phys. Rev. Lett.*, 2014, **113**, 156803.
32 J. C. Greenbank and B. B. Argent, *Trans. Faraday Soc.*, 1965, **61**, 655.
33 L. De Trizio, F. De Donato, A. Casu, A. Genovese, A. Falqui, M. Povia and L. Manna, *ACS Nano*, 2013, **7**, 3997.